

## Supplementary Information

# **Zinc Tin Oxide as High-Temperature Stable Recombination Layer for Mesoscopic Perovskite/Silicon Monolithic Tandem Solar Cells**

J r mie Werner,<sup>1</sup> Arnaud Walter,<sup>3</sup> Esteban Rucavado,<sup>1</sup> Soo-Jin Moon,<sup>3</sup> Davide Sacchetto,<sup>3</sup> Michael Rienaecker,<sup>2</sup> Robby Peibst,<sup>2</sup> Rolf Brendel,<sup>2</sup> Xavier Niquille,<sup>1</sup> Stefaan De Wolf,<sup>1,4</sup> Philipp L per,<sup>1</sup> Monica Morales-Masis,<sup>1</sup> Sylvain Nicolay,<sup>3</sup> Bjoern Niesen,<sup>1,3</sup> and Christophe Ballif<sup>1,3</sup>

<sup>1</sup> *Ecole Polytechnique F d rale de Lausanne (EPFL), Institute of Microengineering (IMT), Photovoltaics and Thin-Film Electronics Laboratory, Rue de la Maladi re 71b, 2002 Neuch tel, Switzerland.*

<sup>2</sup> *Institute for Solar Energy Research Hamelin (ISFH), Germany*

<sup>3</sup> *CSEM, PV-Center, Jaquet-Droz 1, 2002 Neuch tel, Switzerland.*

<sup>4</sup> *Now at: Kaust Solar Center, 4700 King Abdullah University of Science and Technology, Kingdom of Saudi Arabia*

\* Corresponding author e-mail: jeremie.werner@epfl.ch

## Silicon cell fabrication

The silicon bottom cells were fabricated from n-type float-zone wafers (375  $\mu\text{m}$  thick; 15  $\Omega\text{cm}$ ), which were CMP polished on front-side and lapped on rear-side. After a RCA cleaning, a 150-nm-thick  $\text{SiO}_2$  was thermally grown by wet oxidation at 900°C. Hotmelt wax was inkjet printed on the front side to define the active area of the cells, where the oxide layer was etched away with a HF (40%) dip. The wax was removed by washing the samples with isopropanol. BSF regions on the rear-side were defined by local picosecond laser (532 nm) ablation (25  $\mu\text{m}$  spot size; 75  $\mu\text{m}$  spot-to-spot distance). After RCA cleaning, phosphorous ion implantation on the rear-side was carried out at 10 keV (dose 5  $10^{15}$   $\text{cm}^{-2}$ ) and boron ion implantation on the front-side at 5 keV (dose 3  $10^{15}$   $\text{cm}^{-2}$ ), with the oxide layer acting as mask. The samples were then annealed at 1050°C for 80 min in  $\text{N}_2$  atmosphere, followed by a forming gas anneal at 425°C for 30 min.

## Tandem cell fabrication

The tandem cells were fabricated from the silicon bottom cells described above with the following process sequence: Single-junction NIR-transparent 1  $\text{cm}^2$  perovskite solar cells were co-prepared applying steps 3-10 to FTO-coated glass substrates.

1. The silicon wafer samples were first dipped in a 1% hydrofluoric acid solution for 60 seconds to remove the silicon native oxide layer.
2. Then the intermediate recombination layer was formed by sputtering a transparent conducting oxide. ZTO was deposited using a magnetron RF sputtering system with a power density of 0.32  $\text{W}/\text{cm}^2$  at 60 °C, under an atmosphere of argon and oxygen with Ar/O<sub>2</sub> flow ratio of 10/2. More details of the deposition parameters, the material development and application of a-ZTO with this particular stoichiometry are described in detail elsewhere.<sup>1</sup>
3. A 20nm thick sub-stoichiometric  $\text{TiO}_{2-x}$  layer was deposited by sputtering from a ceramic  $\text{TiO}_2$  target at a power of 300W.
4. A mesoporous  $\text{TiO}_2$  layer was subsequently spin coated on the substrates at 4000rpm for 30s to form a scaffold layer from a 1:5 diluted solution in isopropanol.
5. All samples were sintered at 500°C for 15min.
6. After cooling the samples to room temperature, a 320 nm-thick aluminum layer was evaporated on the rear side and annealed at 380°C.
7. The perovskite layer was spin coated on the bottom cells from a 1.4M solution of  $\text{PbI}_2$  (TCI) and  $\text{CH}_3\text{NH}_3\text{I}$  (Dyesol) in DMSO:DMF (Sigma Aldrich) at 1000rpm for 10s, followed by a step at 5000rpm for 45s. Halfway through the second step an anti-solvent treatment was applied using DEE (Sigma Aldrich). The substrates were subsequently dried at 50°C and annealed for 10min at 100°C.
8. A spiro-OMeTAD solution in chlorobenzene (72.3 mg/ml 2,2',7,7'-tetrakis-(N,N-di-4-methoxyphenylamino) -9,9'-spirobi-fluorenes (Merck), 28.8  $\mu\text{l}/\text{ml}$  4-tert-butylpyridine (TCI), 17.5  $\mu\text{l}/\text{ml}$  stock solution of 520 mg/ml lithium bis trifluoromethylsulfonyl imide (Sigma-Aldrich) in acetonitrile) was then spin coated at 4000 rpm for 30 s to form the hole transporting layer.
9. The transparent electrode consisted of a 10-nm-thick thermally evaporated molybdenum oxide buffer layer and a 100-nm-thick sputtered hydrogenated indium oxide and indium tin oxide bilayer (90nm/10nm), having a sheet resistance of about 40  $\Omega/\text{sq}$ .
10. The devices were completed with a thermally evaporated gold frame and, for the larger cells, fingers, to improve the lateral charge transport.

## Characterization

J–V measurements were carried out on a two-lamp (halogen and xenon) class AAA WACOM sun simulator with an AM1.5 g irradiance spectrum at 1000  $\text{Wm}^{-2}$ . Laser-cut shadow masks were used to define the illuminated area, which was then measured with a confocal microscope. The scan rate was fixed at 33 mV/s for all devices. EQE spectra were measured on a custom-made spectral response setup equipped with a xenon lamp, a grating monochromator and lock-in amplifiers, with the light being chopped at a frequency of 10 Hz. Light bias was used to characterize the subcells individually, as also described in more detail elsewhere.<sup>2</sup> The antireflective coating foils were in-house replicates of cubic structures similar to the work of Ulbrich et al.<sup>3</sup> All J–V and EQE measurements were carried out in air, without encapsulation. A stylus profilometer was used to measure the thicknesses of thin films on glass. A UV–vis–NIR spectrophotometer (PerkinElmer Lambda 900) with an integrating sphere was used to acquire the total reflectance, transmittance, and absorbance. The SEM cross-section images were acquired on a JEOL JSM-7500TFE at 2 kV accelerating voltage. Electrical conductivity, carrier Hall mobility and carrier density were obtained from Hall-effect measurements in the van der Pauw configuration on an Ecopia HMS-5000 system.

## References

1. Morales-Masis, M. *et al.* An Indium-Free Anode for Large-Area Flexible OLEDs: Defect-Free Transparent Conductive Zinc Tin Oxide. *Adv. Funct. Mater.* **26**, 384–392 (2016).
2. Werner, J. *et al.* Efficient Monolithic Perovskite/Silicon Tandem Solar Cell with Cell Area >1  $\text{cm}^2$ . *J. Phys. Chem. Lett.* **7**, 161–166 (2016).

3. Ulbrich, C., Gerber, A., Hermans, K., Lambertz, A. & Rau, U. Analysis of short circuit current gains by an anti-reflective textured cover on silicon thin film solar cells. *Prog. Photovoltaics Res. Appl.* **21**, 1672–1681 (2013).
4. Cho, S. H. *et al.* Highly transparent ZTO/Ag/ZTO multilayer electrode deposited by inline sputtering process for organic photovoltaic cells. *Phys. Status Solidi Appl. Mater. Sci.* **211**, 1860–1867 (2014).
5. Morales-masis, M., Nicolas, S. M. De, Holovsky, J., Wolf, S. De & Ballif, C. Low-Temperature High-Mobility Amorphous IZO for Silicon Heterojunction Solar Cells. *IEEE J. Photovoltaics* **5**, 1340–1347 (2015).
6. Löper, P. *et al.* Complex Refractive Index Spectra of CH<sub>3</sub>NH<sub>3</sub>PbI<sub>3</sub> Perovskite Thin Films Determined by Spectroscopic Ellipsometry and Spectrophotometry. *J. Phys. Chem. Lett.* **6**, 66–71 (2015).
7. J.R.DeVore. Refractive Indices of Rutile and Sphalerite. *J. Opt. Soc. Am.* **41**, 416–419 (1951).
8. Schinke, C. *et al.* Uncertainty analysis for the coefficient of band-to-band absorption of crystalline silicon. *AIP Adv.* **5**, (2015).

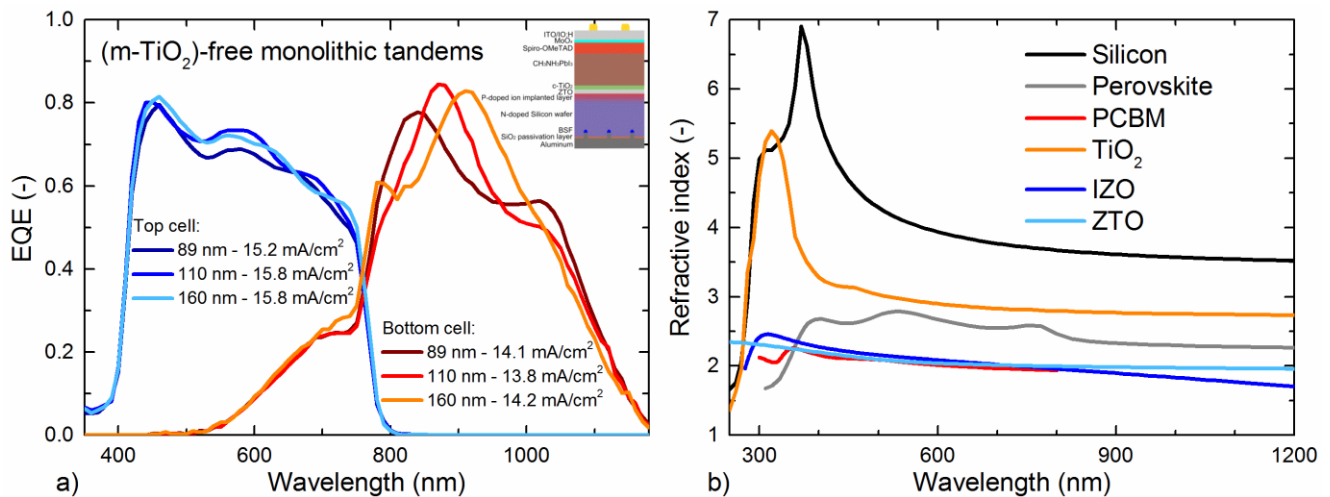


Figure S1 a) EQE curves of monolithic tandem solar cells with three different ZTO thicknesses and without TiO<sub>2</sub> scaffold in the perovskite top cell (as contrast to the cells shown in the main manuscript), showing similar interferences in the silicon cell as the tandem with scaffold layer; b) Refractive indices of the main materials involved around the recombination junction for the present tandem cells and, as comparison, for tandem cells of previous work. The ellipsometric data was taken from the literature.<sup>4-8</sup>

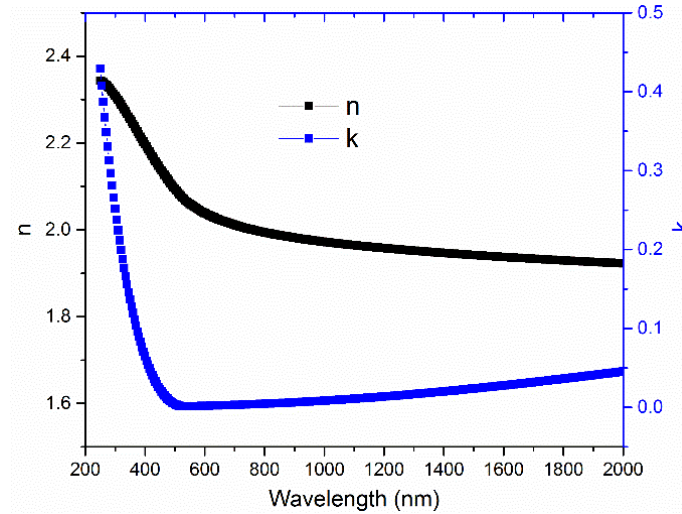


Figure S2 Refractive index and extinction coefficient for 150-nm-thick ZTO layer measured by spectroscopic ellipsometry.

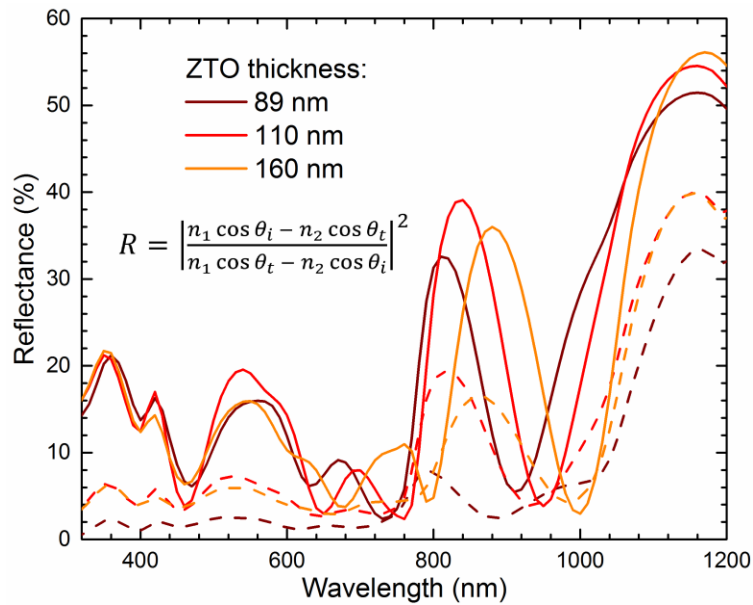


Figure S3 Reflectance curves for three different mesoscopic monolithic tandem cells having different ZTO recombination layer thicknesses. Solid lines are without ARF and dashed lines with ARF. The inset gives the equation for the reflectance at an interface in function of the refractive indices of the two adjacent layers.

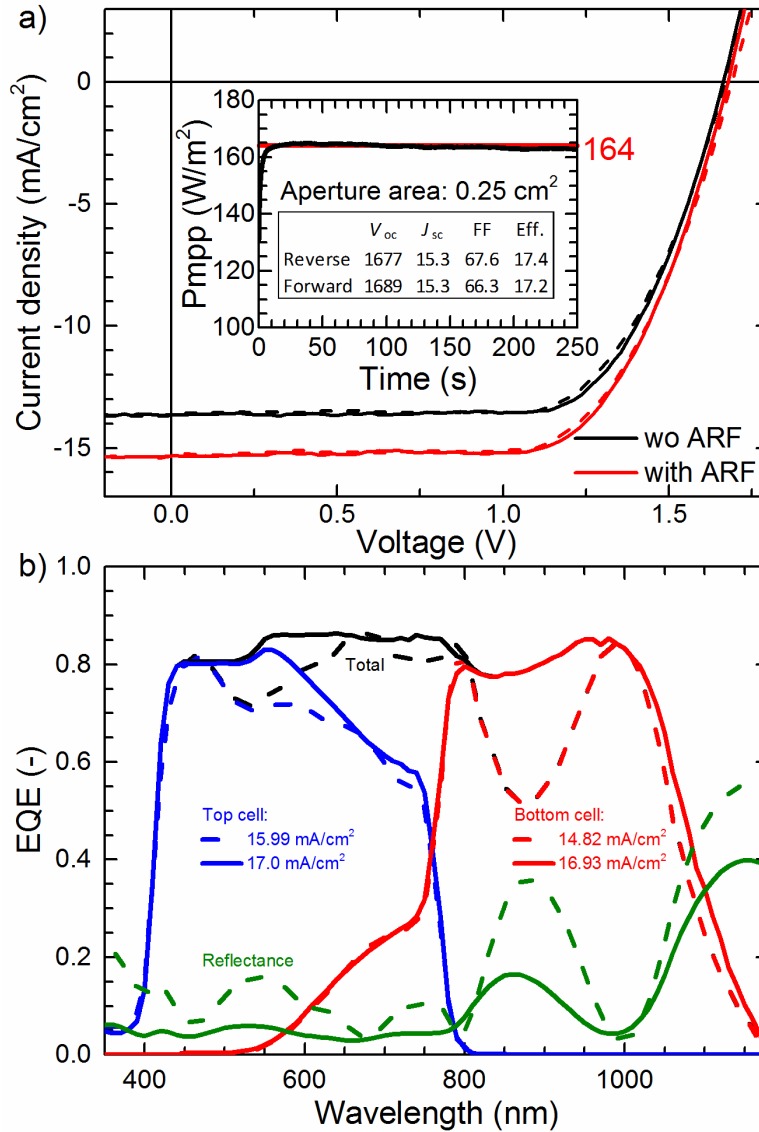


Figure S4 a) J-V measurements of the best performing 0.25 cm<sup>2</sup> monolithic tandem with and without antireflective foil (ARF). The inset shows the steady power output measured under maximum power point tracking; b) EQE and total reflectance measurements of the same device as in a), with (solid lines) and without (dashed lines) ARF. The total curve is the sum of the top and bottom cell responses.

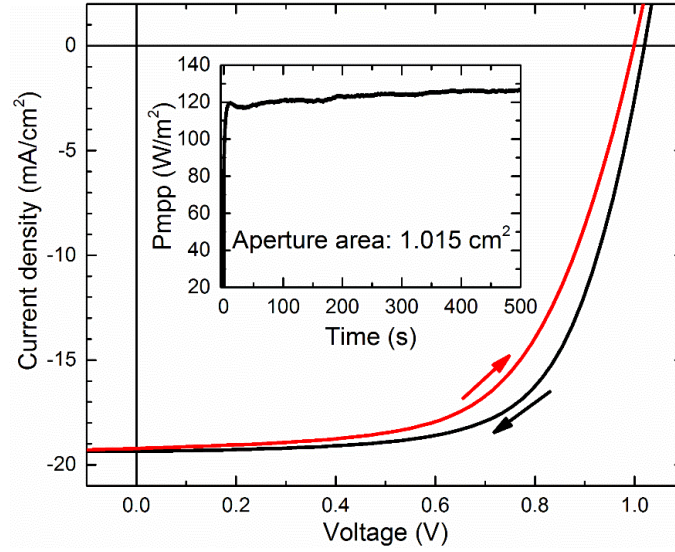


Figure S5 Current-voltage characteristics of a near-infrared transparent mesoscopic perovskite solar cell, fabricated in parallel to the monolithic tandem cells. The inset shows the maximum power point tracking curve.

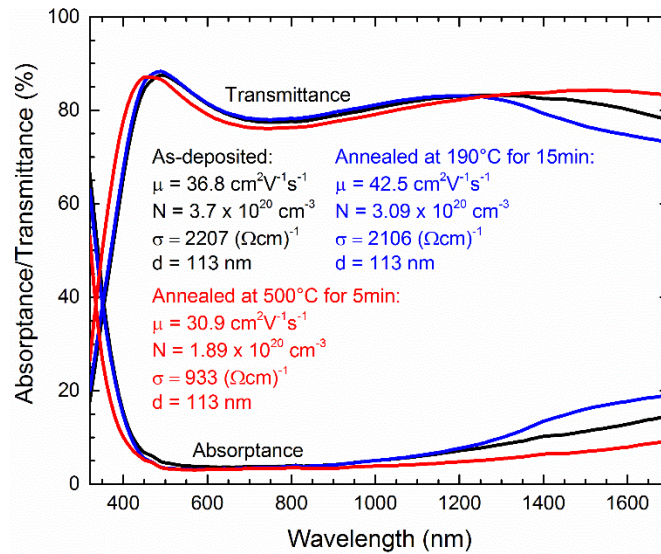


Figure S6 Transmittance and Absorbance of ITO layers on glass: as deposited, annealed at 190°C for 15min and annealed at 500°C for 5min. The Hall effect parameters, including mobility, carrier concentration and conductivity, are given in the tables with the respective colors corresponding to the optical curves. Further annealing the samples at 500°C, as it would be necessary for the top perovskite cell processing, resulted in non-measurable films, likely due to further decrease in conductivity.